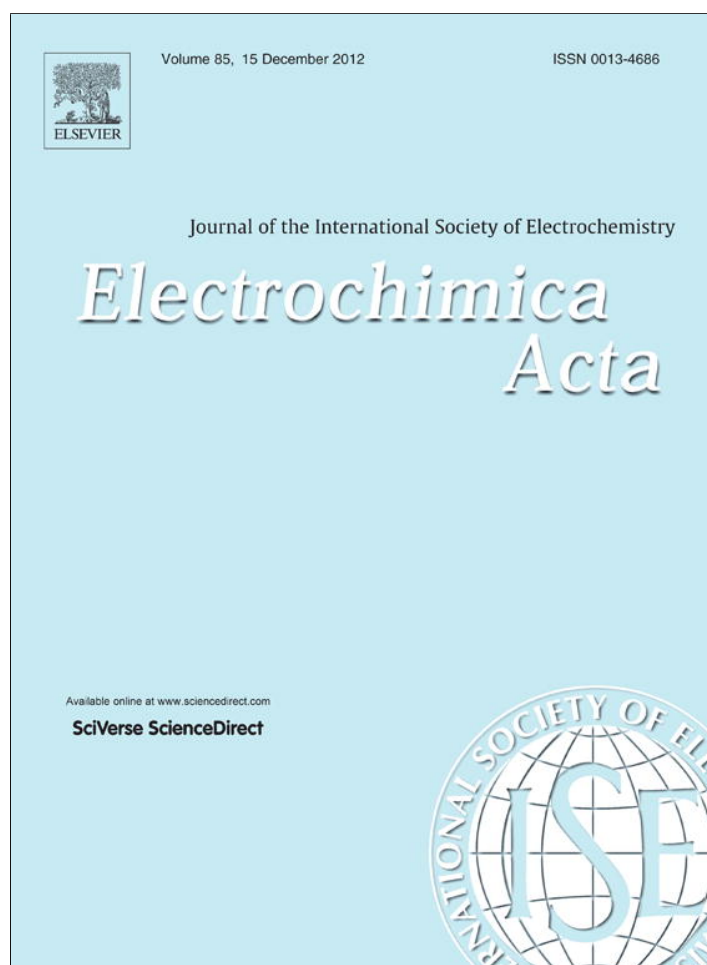


Provided for non-commercial research and education use.
Not for reproduction, distribution or commercial use.



This article appeared in a journal published by Elsevier. The attached copy is furnished to the author for internal non-commercial research and education use, including for instruction at the authors institution and sharing with colleagues.

Other uses, including reproduction and distribution, or selling or licensing copies, or posting to personal, institutional or third party websites are prohibited.

In most cases authors are permitted to post their version of the article (e.g. in Word or Tex form) to their personal website or institutional repository. Authors requiring further information regarding Elsevier's archiving and manuscript policies are encouraged to visit:

<http://www.elsevier.com/copyright>



Carbon nanotube modified carbon cloth electrodes: Characterisation and application as biosensors

Madalina M. Barsan^a, Ricardo C. Carvalho^a, Yu Zhong^b, Xueliang Sun^b, Christopher M.A. Brett^{a,*}

^a Departamento de Química, Faculdade de Ciências e Tecnologia, Universidade de Coimbra, 3004-535 Coimbra, Portugal

^b Department of Mechanical and Materials Engineering, The University of Western Ontario, London, Ontario, Canada N6A 5B9

ARTICLE INFO

Article history:

Received 24 May 2012

Received in revised form 10 August 2012

Accepted 10 August 2012

Available online 20 August 2012

Keywords:

Carbon cloth

Carbon nanotubes

Nitrogen doping

Conducting polymers

Biosensor

ABSTRACT

Carbon nanotubes (CNTs) and nitrogen doped carbon nanotubes (CNx) modified carbon cloth (CCI) materials have been employed for the first time for the development of new electrode sensor materials, and characterised by cyclic voltammetry and electrochemical impedance spectroscopy. The voltammetric response of model electroactive species shows a close to reversible electrochemical behaviour, under diffusion control, at both functionalised CNT.CCI and CNx.CCI. Polymerisation of 3,4-ethylenedioxythiophene (EDOT) at CCI based electrodes was performed in order to decrease the material pore size and decrease sorption. The difference in charge values of PEDOT-modified CCI-based electrodes indicates that different amounts of polymer are deposited at each substrate. Glucose biosensors were constructed by immobilising glucose oxidase on top of PEDOT.CNT/CNx.CCI and the analytical properties together with operational stability were evaluated. Electrochemical impedance spectroscopy was used to evaluate interfacial and bulk properties of CNT/CNx.CCI, PEDOT.CNT/CNx.CCI and GOx.PEDOT.CNT/CNx.CCI electrodes, and differences in both capacitance and charge transfer resistance values are seen, revealing the advantages of CNT and CNx modification of CCI.

© 2012 Published by Elsevier Ltd.

1. Introduction

High performance carbon fibres (CF) were first synthesised by Bacon in 1958 [1], by carbonisation of rayon and their carbon content was increased up to 55% when Shindo produced them from polyacrylonitrile (PAN) [2], application being in aero-engine fabrication. Carbon paper and carbon cloths (CCI), both carbon fibre based porous materials, the first non-woven and the other woven-fabric, are nowadays still made from PAN or petroleum pitch and have become the most effective electrode substrate for polymer electrolyte membrane fuel cells (PEMFCs), due to their good electric conductivity, gas permeability, and corrosion resistance [3,4]. Together with carbon nanotubes, they have been used to improve the electrocatalytic activity and reduce the amount of platinum catalyst [5–10].

Carbon nanotubes (CNTs) deposited on CCI can substantially improve the performance of CCI as substrates for Pt nanoparticles, due to their high aspect ratio and good electronic conductivity. Conventional methods for modifying CCI with CNTs, which consist of inking the substrate with a mixture of CNT powder and solvent [5,11], introduce impurities which degrade the electro-

chemical performance of the device, so that they were substituted by the direct growth of the CNTs on CCI by chemical vapour deposition [12,13]. Nevertheless, their inertness means that surface functionalisation is necessary to ensure effective reactivity and attachment of nanoparticles or biomolecules. Functionalisation by chemical oxidation (acid treatment) reduces the mechanical and electronic performance, and the introduction of surface defects makes adsorption non-uniform [14]. Doping is another way to functionalise CNTs, by introducing nitrogenated sites (substitutional and pyridinic oxygen), formed during nitrogen incorporation into the CNT lattice, while distorted graphene layers bond around nitrogen defects. This gives nitrogen doped CNTs (CNx) a bamboo-like appearance [15], also known as polymerised carbon nitride nanobells [16].

Besides the advantages of using CNTs and CNx modified CCI in proton exchange membrane fuel cells, both modifiers give potentially interesting substrates for protein adsorption for bio-device applications. Proteins can adsorb strongly by non-covalent linkage, along the lengths of CNTs, e.g. streptavidin [17], ferritin [18], cytochrome c [19], or antibodies [20]. The structure-dependent metallic character of multiwalled carbon nanotubes should enable them to promote electron-transfer reactions at low overpotentials and thence, together with their high surface area, make them excellent for application in biochemical sensing systems, for example amperometric glucose biosensors [21]. CNx presents

* Corresponding author. Tel.: +351 239 835295; fax: +351 239 835295.

E-mail address: brett@ci.uc.pt (C.M.A. Brett).

some advantages over un-doped CNTs, such as higher conductivity, lower toxicity, and the presence of nitrogen sites [22], which have been shown to facilitate electron transfer between metalloproteins and Au-electrodes [23].

This paper reports, for the first time, the use of CNT and CNx modified CCl (CNT.CCl, CNx.CCl), as substrates for glucose biosensor construction. Carbon cloths have been reported as substrates for direct-growth of PANI nanowires (PANI-NWs), and the enzyme glucose oxidase was immobilised via electrostatic interaction between the positively charged (oxidised) NW-surface and the negatively charged GOx molecules [24]. Another application of CCl was the preparation of a FAD-dependent glucose dehydrogenase anode and bilirubin oxidase cathode for biofuel cells, in which enzymes were deposited together with a carbon ink [25]. In this work, the electrochemical behaviour of CNT and CNx modified CCl was first characterised by cyclic voltammetry, using the model electroactive species, $K_4Fe(CN)_6$, also estimating the electroactive area. Due to the high porosity, and their high liquid adsorption capacity through capillarity, modifying the CCl based electrodes with an inert conducting polymer is needed, in order to reduce the pore diameter. For this purpose, poly(3,4-ethylenedioxythiophene) (PEDOT) is attractive because films can be easily deposited by monomer electropolymerisation [26], and have high conductivity and good stability under ambient conditions [27,28]. Such PEDOT-modified CNT.CCl or CNx.CCl were used as glucose biosensors, with immobilised glucose oxidase (GOx), designated GOx.PEDOT.CNT/CNx.CCl, by fixed potential amperometry, at low overpotential. Electrochemical impedance spectroscopy was also employed to evaluate interfacial and bulk characteristics of the CNT/CNx.CCl, PEDOT.CNT/CNx.CCl and GOx.PEDOT.CNT/CNx.CCl electrodes.

2. Experimental

2.1. Reagents and solutions

The CNTs and CNx were synthesised by CVD method in a quartz tube mounted in a hot-wall furnace [29]. Carbon papers were used as the substrates and placed at the centre of the tube. The substrates were pre-treated by depositing a very thin Fe film with 5 nm in thickness which acted as catalyst. An Ar flow (300 sccm) was used as carrier gas and the tube was purged for 15 min before reaction. For the synthesis of CNTs, when the system was heated up to required temperature (760 °C), C_2H_4 (50 sccm) was introduced into the reaction zone, and the growth of CNTs happened at the surface of the substrates for 15 min. After reaction, the system was cooled down to room temperature. For the synthesis of CNx, melamine was the only source of carbon and nitrogen precursors, and placed near the entrance of the furnace. At the required synthesis temperature (800 °C), melamine was evaporated and transported to reaction zone to initiate the growth of CNx on the substrate. The reaction was held for 15 min and terminated. Then the system was cooled down to room temperature.

For the evaluation of the electroactive areas, a standard 3 mM potassium hexacyanoferrate (II) (Fluka, Switzerland) solution was prepared by dissolving the salt in 0.1 M potassium chloride electrolyte solution.

The monomer 2,3-dihydrothieno[3,4-b]-1,4-dioxin (EDOT) was from Aldrich, Germany and the solution used for the polymerisation contained 0.01 M of monomer dissolved in 0.1 M 4-styrenesulfonic acid sodium salt hydrate (NaPSS, Aldrich, Germany).

Bovine serum albumin (BSA), glutaraldehyde (GA) 25% (v/v) and α -D(+)-glucose were from Sigma-Aldrich, Germany and glucose oxidase (GOx, EC 1.1.3.4, from *Aspergillus niger*, 24 units/mg) was from Fluka, Switzerland.

For electrochemical experiments, the supporting electrolyte was 0.1 M KCl or sodium phosphate buffer saline (NaPBS) (0.1 M phosphate buffer + 0.05 M NaCl, pH = 7.0), prepared from sodium di-hydrogenphosphate, di-sodium hydrogenphosphate (both from Fluka, Germany) and sodium chloride (Riedel-de-Haën, Germany). A stock solution of 0.1 M glucose (Sigma, USA) was prepared in 0.1 M NaPBS at least one day before use, to permit equilibration of α and β anomers of D-glucose and was then kept in the refrigerator and used within one week.

Millipore Milli-Q nanopure water (resistivity $\geq 18 M\Omega cm$) and analytical reagents were used for the preparation of all solutions. Experiments were performed at room temperature, 25 ± 1 °C.

2.2. Instrumentation

A three-electrode electrochemical cell of 10 cm³ volume was used, containing the CNT.CCl or CNx.CCl-based electrodes as working electrodes, a platinum foil counter electrode and a saturated calomel electrode (SCE) as reference.

Electrochemical measurements and electrochemical impedance spectroscopy (EIS) experiments were carried out by a potentiostat/galvanostat/ZRA, (Gamry Instruments, Reference 600). For EIS experiments, an rms perturbation of 10 mV was applied over the frequency range 100 kHz–0.1 Hz, and 10 frequency values per decade. The spectra were recorded at open circuit potential (OCP).

The pH-measurements were done with a CRISON 2001 micro pH-meter.

2.3. Electrode and biosensor preparation

Electrodes were fabricated by cutting the modified CCl in 1.0 cm \times 0.5 cm rectangles, and fixing one end of the rectangle to an electrical connector, originally designed to connect Au quartz crystals.

For electropolymerisation of EDOT, a 0.01 M monomer solution was freshly prepared by dissolving the monomer in 0.1 M NaPSS, and the solution was heated until complete monomer dissolution. EDOT was electropolymerised by potential cycling from –0.6 up to 1.2 V vs. SCE for 10 cycles at a scan rate of 50 mV s^{–1}, a procedure optimised in [26]. PEDOT films were allowed to dry in air at room temperature, for at least 24 h, before use.

Glucose oxidase was immobilised on top of PEDOT-modified CCl.CNT/CNx electrodes by cross-linking with glutaraldehyde (GA) as reported in [30]. A volume of 20 μ l of enzyme solution was mixed with 10 μ l GA (2.5%, v/v diluted in water) and 20 μ l of this mixture was then dropped onto the electrode surface and left to dry at room temperature during at least 4 h.

3. Results and discussion

3.1. Determination of electroactive areas of CCl, CNT.CCl and CNx.CCl electrodes

Cyclic voltammograms were recorded at all three types of CCl based electrodes in 0.1 M KCl, and it was observed that the more resistive material is the unmodified CCl, see inset in Fig. 1a. As expected, the CNT modification of CCl leads to an increase of the material's capacitance, reflected in the higher capacitive currents, the largest being that of the nitrogen doped CNT, CNx. The charge values were also calculated by integrating the current of the corresponding CV-s and the CNx.CCl had a charge value of 7.2 mC cm^{–2}, higher by a factor of 1.6 and 16 than those of CNT.CCl and CCl electrodes, respectively.

In order to investigate further the electrochemical properties of CCl-based electrodes, the diffusion-controlled electrode reaction of hexacyanoferrate(II) in 0.1 M KCl solution was investigated

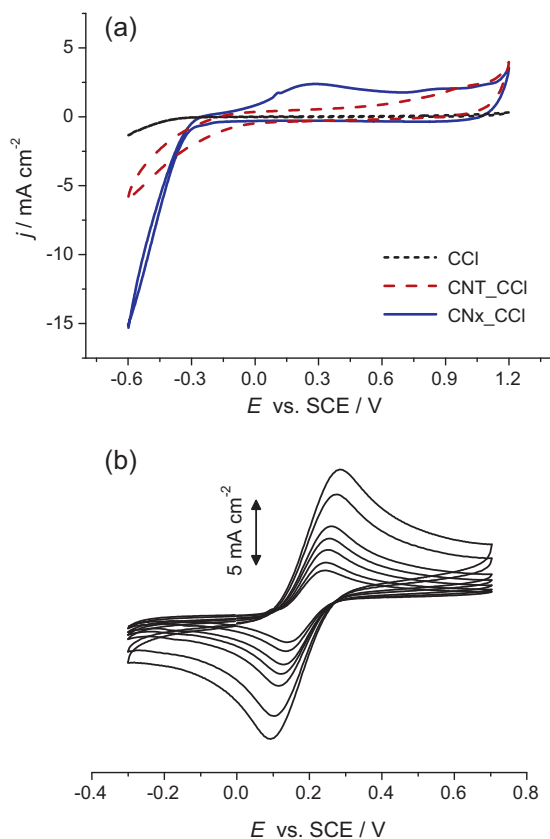


Fig. 1. Cyclic voltammograms recorded at bare CCI, CNT_CCI and CNx_CCI electrodes (a) in 0.1 M KCl at $\nu = 50 \text{ mV s}^{-1}$ and (b) 0.1 M KCl containing 3 mM $\text{K}_4\text{Fe}(\text{CN})_6$; scan rate 10 up to 150 mV s^{-1} .

by cyclic voltammetry. First, experiments were made using the cloth samples without any functionalisation. It was observed, due to their hydrophobic nature, that there was no electrochemical response towards the oxidation of $[\text{Fe}^{\text{II}}(\text{CN})_6]^{4-}$, at CCI and CNT_CCI electrodes, and an irreversible response at CNx_CCI, which have a less hydrophobic character, due to their functionalisation with nitrogen. Therefore, the electrodes were functionalised, by immersion in 2 M HNO_3 during 24 h, afterwards being rinsed with water and dried at 50°C for another 24 h. This procedure made the surface of the electrodes more hydrophilic, excepting for CCI which remained hydrophobic, and required an immersion of 10 min in the hexacyanoferrate(II)-containing solution prior to the CV experiment. Even so, poorly defined peaks were observed and the electroactive species had an irreversible redox behaviour, with a peak separation larger than 120 mV. On the contrary, a pair of well-defined redox peaks of the $\text{Fe}(\text{CN})_6^{4-}/\text{Fe}(\text{CN})_6^{3-}$ was obtained at CNT_CCI and CNx_CCI electrodes (see Fig. 1b), with a formal potential (E^0), estimated from the mid-point value of the anodic and cathodic peak potentials, $(E_{\text{pa}} + E_{\text{pc}})/2$, of $\approx 0.18 \text{ V}$ vs. SCE at both electrodes.

Cyclic voltammetry was performed over a range of different scan rates, from 10 up to 150 mV s^{-1} , both cathodic and anodic peak currents depending linearly on the square root of scan rate ($r^2 = 0.998$) over the whole range examined, which indicates that the electrochemical process is diffusion-controlled.

The electroactive surface (A_{ele}) areas of the CNT/CNx_CCI electrodes were calculated according to the Randles–Sevcik equation, and using this value of A_{ele} , standard electron transfer rate constants, k_0 , were deduced. Results are presented in Table 1 and, as seen, CNT and CNx modification of the CCI both lead to a significant increase in the electroactive area. Moreover, the functionalisation

Table 1

Electroactive area (A_{ele}), ratio of electroactive area to geometric area (A_{geo}) of the CCI, CNT/CNx_CCI electrodes, and standard electron transfer rate constants, calculated from cyclic voltammograms recorded in the scan rate range $10\text{--}150 \text{ mV s}^{-1}$, in 0.1 M KCl containing 3 mM $\text{K}_4\text{Fe}(\text{CN})_6$.

	CCI	CNT_CCI	CNx_CCI
A_{ele} (cm^2)	0.08	0.54	0.77
$A_{\text{ele}}/A_{\text{geo}}$	0.32	2.13	3.52
$k_0 \times 10^3$ (cm s^{-1})	0.13	1.72	3.71

of CNx increases the electroactive area the most, with the highest ratio of electroactive to geometric area ($A_{\text{ele}}/A_{\text{geo}}$) of 3.52, compared with 2.13 for CNT_CCI and 0.32 for CCI.

3.2. Electropolymerisation of EDOT on CCI, CNT_CCI and CNx_CCI

One of the drawbacks of CCI-based electrodes during long experiments is their high porosity, due to which electrolyte can reach the electrical contact through capillarity. Short-time experiments, like cyclic voltammetry, imply the immersion of the CCI-based electrodes for only a few minutes, so that there are no problems in wetting the electrical contact. In order to evaluate the period of time required for the contact to be wetted, the CCI-based electrodes were immersed in electrolyte solution and it was observed that after 200 s electrolyte reached the electrode-metal contact.

A way to decrease the capillarity is to decrease the porosity of the material by filling the material with a conducting polymer, such as PEDOT, whose function is electron conduction. Electropolymerisation of EDOT was carried out by potential cycling from a solution containing 0.01 M EDOT dissolved in 0.1 M NaPSS, and a typical CV profile during polymerisation is presented in Fig. 2a. The upper potential limit was +1.2 V, chosen since it was observed that this is the optimum potential required to generate enough radical cation species $\text{EDOT}^{\bullet+}$, which initiate the electropolymerisation process [26]. The increase in the capacitive current is an indication that PEDOT polymer is formed. A comparison of the CV responses of PEDOT modified CCI-based electrodes is presented in Fig. 2b.

PEDOT deposition at CCI-based electrodes leads to different increases of the capacitive charge relative to the bare electrodes. The charge values were calculated from the CV recorded at PEDOT modified CCI, CNT_CCI and CNx_CCI modified electrodes in 0.1 M KCl, and are shown in Table 2. The highest increase in charge was observed for PEDOT_CCI, the value being 6.9, compared with 0.45 mC cm^{-2} at bare electrodes. The highest charge value of 66.5 mC cm^{-2} was recorded at PEDOT_CNx_CCI, followed by PEDOT_CNT_CCI, with 24.2 mC cm^{-2} , being 10 and 6 respectively times greater than that recorded at the bare electrodes.

3.3. Biosensors based on PEDOT modified CCI, CNT_CCI and CNx_CCI

3.3.1. Optimisation of the immobilisation method of the enzyme

Considering the high porosity of the PEDOT modified CCI based electrodes, the first method used to immobilise the enzyme was by physical adsorption. The major advantage of this method is that requires no additional reagents, and causes little, or no

Table 2

Charge values (Q (mC cm^{-2})), calculated integrating the current of the corresponding voltammograms recorded at bare, PEDOT modified and at PEDOT modified CCI based biosensors in 0.1 M KCl; $\nu = 50 \text{ mV s}^{-1}$.

	Bare CCI	PEDOT_CCI	GOx_PEDOT_CCI
CCI	0.5	6.9	3.2
CNT_CCI	4.3	24.2	12.9
CNx_CCI	7.2	66.5	33.4

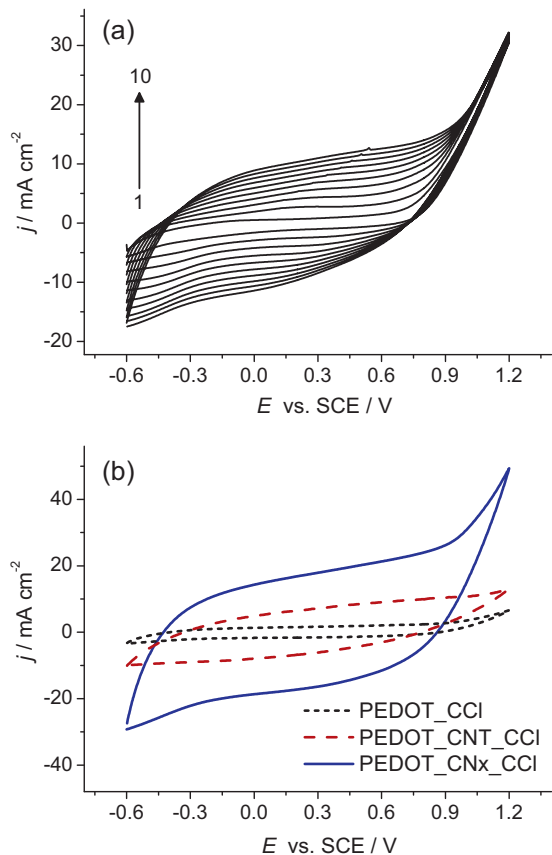


Fig. 2. (a) Typical CV-s recorded during EDOT polymerisation at CCI based electrodes and (b) cyclic voltammograms recorded at CCI, CNT.CCI and CNx.CCI PEDOT modified electrodes in 0.1 M KCl; $\nu = 50 \text{ mV s}^{-1}$.

conformational changes to the enzyme. The substrates were immersed in a 1% (w/v) GOx solution, during 30 min at room temperature. They were then immersed in water, in order to remove the excess of weakly adsorbed enzyme and were allowed to dry during 4 h before use.

The biosensors were used for glucose detection by fixed potential amperometry at -0.45 V vs. SCE . No glucose response was observed at the PEDOT.CCI biosensor, while PEDOT.CNT.CCI and PEDOT.CNx.CCI exhibit similar sensitivities, of 9.0 ± 0.6 ($n = 3$). Unfortunately, the response decreased drastically and was lost after only 3 measurements, probably due to the weak binding forces between the enzyme and the substrate, mainly hydrogen bonds, multiple salt linkages, and Van der Waal's forces.

Thus, the enzyme was chemically immobilised by crosslinking with GA, using a 1% GOx solution which contained 4% of BSA. The biosensor constructed by this method exhibited a good response up to 1 mM, and was stable during one week of testing and was thus chosen for further biosensor fabrication.

3.3.2. Optimisation of the applied potential for amperometric detection

Fixed potential amperometric detection of glucose was carried out at applied potentials in the range from -0.5 to 0.0 V , in order to determine which potential led to the best biosensor response. First, a full concentration range calibration curve was recorded at -0.45 V , chosen taking into account the formal potential of the enzyme cofactor FAD, $E^0 = -0.45 \text{ V vs. SCE}$ [31]. The response was linear up to approximately 1 mM, so it was decided to inject a concentration of 0.4 mM of glucose at all applied potentials mentioned above, and calculate the change in current (see Fig. 3). In all cases an

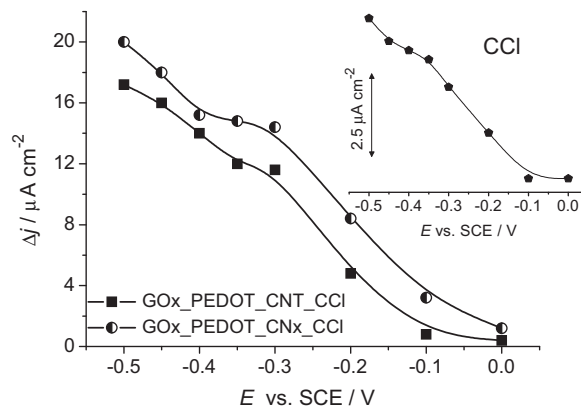


Fig. 3. Variation of PEDOT modified CCI based biosensor response with applied potential; Δj corresponds to the injection of 0.4 mM of glucose in 0.1 M NaPBS pH 7.0.

increase in anodic current occurred. Higher currents were recorded at potentials around the FAD/FADH₂ formal potential, as expected, and as the potential became more positive, the change in current continuously decreased. The CCI and CNT.CCI biosensors lost all response at 0.0 V vs. SCE . The most important result was that no significant variation in current response was observed between -0.4 V and -0.3 V , and therefore -0.3 V was chosen for further experiments, since less negative potentials should lessen any response from reduction of interfering species.

3.3.3. Analytical properties of biosensors based on PEDOT modified CCI, CNT.CCI and CNx.CCI

Using the best conditions tested above, the GOx.PEDOT.CCI and GOx.PEDOT.CNT/CNx.CCI biosensors were therefore employed for amperometric glucose determination at -0.3 V vs. SCE ; calibration curves are displayed in Fig. 4. Since the substrate influenced the PEDOT deposition, it also plays an important role in biosensor performance. As expected, the CNx.CCI substrate, which also led to the best EDOT polymerisation, gives the best analytical properties, with the highest sensitivity of $47.9 \pm 3.5 \mu\text{A cm}^{-2} \text{ mM}^{-1}$ (RSD = 7.3%, $n = 3$), the lowest detection limit of 16 nM and largest linear range. As observed by comparing the sensitivities of the three different substrates (Table 3) the CNT and CNx modification of CCI considerably enhanced the biosensor response, the sensitivities being ≈ 10 times higher than those exhibited by the GOx.PEDOT.CCI biosensor.

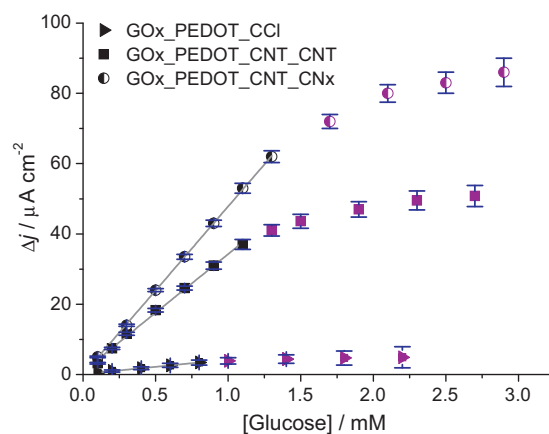


Fig. 4. Calibration curves recorded at GOx.PEDOT modified CCI based biosensors in 0.1 M NaPBS pH 7.0; applied potential -0.3 V vs. SCE .

Table 3

Analytical parameters extracted from the calibration curves recorded at CCl based biosensors, presented in Fig. 4.

	Sensitivity ($\mu\text{A mM}^{-1} \text{cm}^{-2}$)	Detection limit (nM)	K_M (mM)
GOx_PEDOT_CCl	4.1 ± 0.3	22.0 ± 0.6	0.43 ± 0.05
GOx_PEDOT_CNT_CCl	33.4 ± 2.5	65.0 ± 4.7	0.61 ± 0.04
GOx_PEDOT_CNx_CCl	47.9 ± 3.5	16.0 ± 1.1	0.74 ± 0.06

3.3.4. Stability of GOx_PEDOT_CNT/CNx_CCl biosensors

A stability study of the newly developed biosensors was necessary to evaluate the retention of enzyme activity in this biosensor architecture. For this purpose, GOx_PEDOT_CNT/CNx_CCl biosensors were tested over a period of 40 days, recording 7-point calibration curves approximately every 3 days. Biosensors were stored in air, at 4 °C, when not used. The variation of the sensitivities with time is presented in Fig. 5. As observed, there is an increase in the sensitivity after the first 3-day period, correlated with conformational changes of the enzyme in the biosensor structure, and probably due to better electronic contact between the PEDOT_CNT/CNx wires with the active centre of the enzyme. After 40 days, the GOx_PEDOT_CNT_CCl sensitivity decreased by 40% but by only 25% when the biosensor architecture contained CNx. This is probably due to the material hydrophilicity, which enables GOx molecules to penetrate the CCl structure when the enzyme solution is dropped on the electrode surface. Moreover, the fact that it was not necessary to store the biosensors in solution also brings advantages, eliminating possible enzyme leaching.

The storage stability of GOx_PEDOT_CNT/CNx_CCl biosensors was also evaluated, recording a full calibration plot after 45 days of storage in air at 4 °C. The sensitivity decreased by 11% and 6% respectively, demonstrating that, under these conditions, carbon cloth modified substrates enable very good preservation of enzyme activity.

3.4. Electrochemical impedance spectroscopy characterisation of bare, PEDOT and GOx_PEDOT coated carbon cloth electrodes

Complex plane impedance spectra recorded at CCl, CNT_CCl and CNx_CCl electrodes in 0.1 M KCl are shown in Fig. 6a. All spectra are dominated by capacitive lines and the presence of CNTs leads to a decrease of the imaginary part of the impedance ($-Z''$) by a factor of 40, suggesting the increase in the capacitance that improves electrochemical response. This was also observed by comparing the cyclic voltammograms recorded at these electrodes, the higher capacitive currents being recorded at CNx_CCl (Fig. 2b).

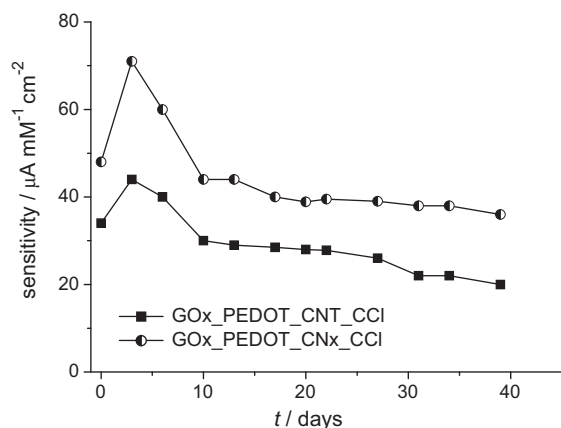


Fig. 5. Stability of GOx_PEDOT_CNT/CNx_CCl biosensors, represented as the sensitivity variation in time.

The PEDOT modified electrodes show a smaller deviation from capacitive behaviour (Fig. 6b), indicating fast electron transfer at the electrode/polymer and polymer/solution interfaces, as well as fast charge transport in the polymer matrix. It was estimated that the actual surface area of a nodular polypyrrole film was 50 times greater than that of a smooth electrode of identical lateral dimensions [32]. In this work dealing with more porous substrates, polymerisation will not occur in a 2-dimensional way but instead will be tridimensional, with the polymer penetrating into the cloth electrode instead of coating only the surface. The decrease of the magnitude of the impedance values observed for the PEDOT modified electrodes shows that the presence of this tridimensional polymer matrix leads to an increase of the total active surface area, in this way increasing the electrical conductivity of the modified electrodes. The difference in the imaginary impedance values obtained for CCl and PEDOT_CCl is not as large as that between bare and PEDOT_CNT/CNx_CCl indicating that PEDOT significantly improves the conductivity of the bare CCl electrodes. The fact that the impedance values are 4 and 10 times lower for PEDOT_CNT_CCl and PEDOT_CNx_CCl respectively, indicates that nanotubes improve the electrochemical response, due to an increase of the electrochemically active area and due to their electrocatalytic behaviour [33], the best being PEDOT_CNx_CCl, owing to CNT nitrogen doping. It has also been reported that the presence of carbon nanotubes increases the number of active sites, compared with PEDOT films deposited on smooth surfaces [34].

Fig. 6c shows spectra of the GOx_PEDOT carbon cloth biosensors, which are very similar to those recorded at PEDOT-modified electrodes, the enzyme layer not significantly affecting the electrochemical behaviour of the carbon cloth based electrodes.

Different circuits were tested to fit the impedance spectra, by non-linear least squares fitting, and that shown in Fig. 6d was found to give an excellent fit, with an average error (χ^2) for the different modifications of $<5 \times 10^{-4}$. All the experimental plots are represented with the respective theoretical fitting.

The complex plane plots at PEDOT modified CCl electrodes (see Fig. 6b), present two distinct regions, corresponding to a finite-length Warburg diffusion impedance in the high and medium frequency ranges and a nearly vertical line which represents a capacitive region in the low frequency range, similar to that observed in [35] for a PEDOT-modified platinum electrode. The equivalent circuit consists of a cell resistance (R_S), a finite-length Warburg diffusion element (Z_D) and a constant phase element (CPE_d) as non-ideal capacitance (a pure capacitor was used in [35]). The Warburg diffusional element, Z_D , is described by the equation: $Z_D = R_D[\text{ctg}(j\omega\tau_D)]^{1/2}/(j\omega\tau_D)^{1/2}$ and is characterised by a diffusional time constant (τ_D), a diffusional pseudocapacitance (C_D) and a diffusion resistance ($R_D = \tau_D/C_D$) [36]. CPE_d was modelled as a non-ideal capacitor, given by $\text{CPE} = -1/(Ci\omega)^\alpha$, where C is the capacitance, which describes the charge separation at the double layer interface, ω is the frequency in rad s^{-1} and the α exponent is due to the heterogeneity of the surface.

As expected, the C_D values increased for the PEDOT_CNT/CNx_CCl modified electrodes, being 49.5 mF cm^{-2} and 631.8 mF cm^{-2} respectively, compared with 19.0 mF cm^{-2} at PEDOT_CCl. The doping had also an effect on the electrode surface morphology, demonstrated by the increased of α value from 0.8 to 0.9, showing that the PEDOT_CNx_CCl electrode has a smoother surface. It was necessary to invoke a non-uniform surface in order to justify the deviation from the ideal 45° phase angle line for infinite diffusion at high and intermediate frequencies; in this way the quality of the fit was significantly improved. In order to fit the spectra recorded at PEDOT_CCl, an equivalent circuit was used containing a pure C instead of a CPE_d , which is the model circuit for PEDOT modified electrodes [35]. In this case, the total bulk

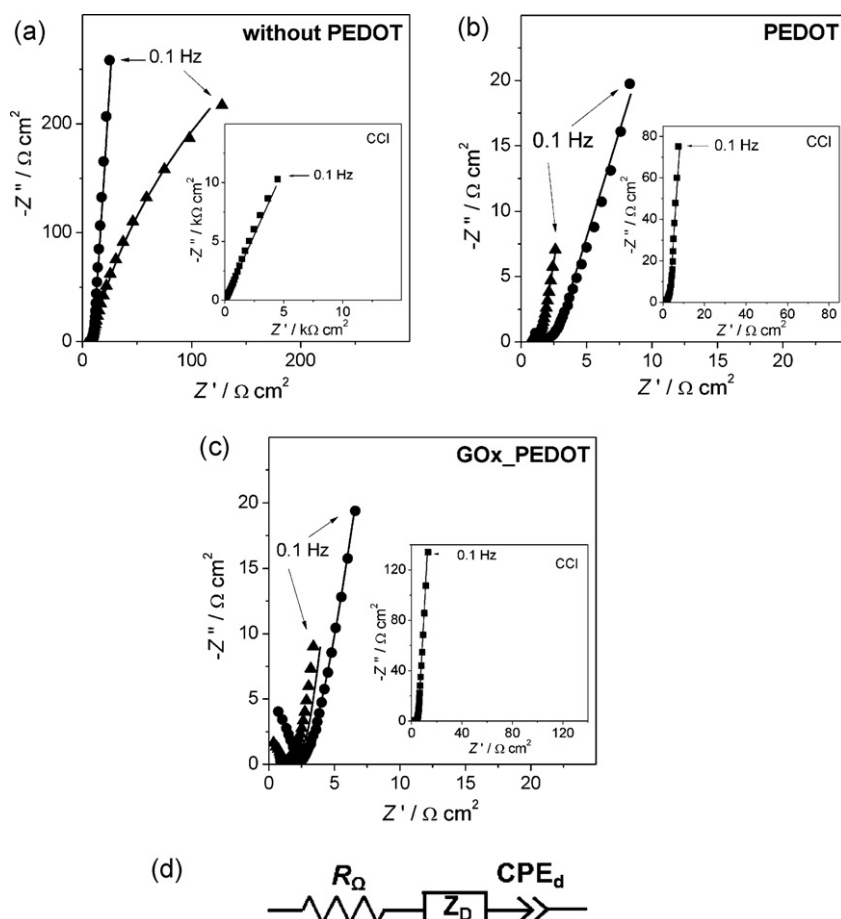


Fig. 6. Complex plane electrochemical impedance spectra in 0.1 M KCl at OCP at (a) no PEDOT, (b) PEDOT modified and (c) GOx.PEDOT-modified electrodes; (■) CCI, (●) CNT.CCI and (▲) CNx.CCI; (d) equivalent circuit used to fit the spectra.

Table 4
Resistance (R_D), τ_D , capacitance (C_D) constant phase element (CPE) and α values and obtained by fitting the EIS spectra from Fig. 6 with the equivalent circuit corresponding to CCI, PEDOT and GOx.PEDOT modified CCI electrodes.

	CCI			PEDOT.CCI			GOx.PEDOT.CCI		
	CCI	CNT.CCI	CNx.CCI	CCI	CNT.CCI	CNx.CCI	CCI	CNT.CCI	CNx.CCI
R_D ($\Omega \text{ cm}^2$)	–	–	–	4.2	2.6	2.0	6.9	3.6	2.4
τ_D (s)	–	–	–	0.04	0.13	1.30	0.13	0.09	0.80
C_D (mF cm^{-2})	–	–	–	10.0	49.5	631.8	19.0	25.2	331.9
CPE ($\text{mF cm}^{-2} \text{ s}^{\alpha-1}$)	0.13	4.05	5.80	–	93.1	360.5	–	101.0	204.0
α	0.73	0.81	0.86	–	0.80	0.90	–	0.81	0.92

capacitance of the polymer was represented by the diffusional element alone, as presented in Table 4.

Due to the highly capacitive response of the bare CCI and CNT/CNx.CCI, the equivalent circuit used to fit the spectra from Fig. 6a, was composed of the cell resistance (R_Ω) and a constant phase element (CPE_d). Observing the CPE_d values presented in Table 4, the influence of CNT is easily noticeable, leading to an increase in the capacitance values by a factor of ≈ 30 for CNT and ≈ 43 for CNx in comparison with bare CCI.

The electrical conductivity is the most important property for an electrochemical biosensor and the low R_D values of 6.9, 3.6 and $2.4 \Omega \text{ cm}^2$ (see Table 4) of GOx.PEDOT.CCI, GOx.PEDOT.CNT.CCI and GOx.PEDOT.CNx.CCI respectively, presented in Table 4, confirm the good electrical conductivity of the biosensors. As expected, the enzyme layer leads to a slight decrease in the overall conductivity, due to the presence of an additional diffusion layer, in which the GOx macromolecules may hinder electron transfer [37]. The most important is that the overall electrochemical

behaviour of the PEDOT modified CCI electrodes is not changed by the enzyme layer deposition, and the low resistance values are promising for fast kinetics of enzymatic reactions to occur.

4. Conclusions

The electrochemical behaviour of carbon nanotube and nitrogen doped carbon nanotube modified carbon cloth materials has been investigated and compared. Model electroactive species show a close to reversible electrochemical behaviour at the functionalised CNT.CCI and CNx.CCI electrodes, the doping of CNT leading to an increase in the electroactive area. Electrodeposition of EDOT at CCI-based electrodes reduces their porosity and increases conductivity, a larger amount of polymer being deposited at CNx.CCI, indicated by the higher amount of charge calculated from cyclic voltammograms. The immobilisation of GOx on the PEDOT.CNT.CCI and PEDOT.CNx.CCI substrates leads to very robust biosensors, those

containing CNx exhibiting the highest sensitivity and lowest detection limit, underlying again the importance of CNT doping. The good stability indicates the advantages in using these porous substrates for retaining enzyme activity, and the possibility of dry storage brings further benefits, as it impedes enzyme leaching. Impedance spectra are in agreement with cyclic voltammetry, CNx.CCl having a higher capacitance than CNT.CCl. The polymerisation of EDOT in the 3D matrix of CCl leads to a significant decrease in charge transfer resistance, lower for PEDOT.CNx.CCl. The two types of biosensors have similar interfacial properties, the enzymatic layer slightly increasing the charge transfer resistance.

Acknowledgements

Financial support from Fundação para a Ciência e a Tecnologia (FCT), Portugal, PTDC/QUI-QUI/116091/2009, POCI 2010 and COM-PETE (co-financed by the European Community Fund FEDER) and CEMUC[®] (Research Unit 285), Portugal, is gratefully acknowledged. MMB thanks FCT for postdoctoral grant SFRH/BPD/72656/2010 and RCC for the doctoral grant SFRH/BD/46496/2008. The research from Canada was supported by Natural Sciences and Engineering Research Council of Canada (NSERC) and Canada Research Chair (CRC) Program.

References

- [1] R. Bacon, *Journal of Applied Physics* 31 (1960) 283.
- [2] E. Fitzer, *Carbon* 27 (1989) 621.
- [3] S. Litster, G. McLean, *Journal of Power Sources* 130 (2004) 61.
- [4] K. Hiroshi, Gas diffusion layer for solid polymer electrolyte fuel cell, U.S patent 6127059.
- [5] W. Li, C. Liang, J. Qiu, W. Zhou, H. Han, Z. Wei, G. Sun, Q. Xin, *Carbon* 40 (2002) 791.
- [6] D.B. Buchholz, S.P. Doherty, R.P.H. Chang, *Carbon* 41 (2003) 1625.
- [7] B. Rajesh, V. Karthik, S. Karthikeyan, K. Ravindranathan Thampi, J.-M. Bonard, B. Viswanathan, *Fuel* 81 (2002) 2177.
- [8] H. Tang, J.H. Chen, Z.P. Huang, D.Z. Wang, Z.F. Ren, L.H. Nie, Y.F. Kuang, S.Z. Yao, *Carbon* 42 (2004) 191.
- [9] H.Q. Hou, D.H. Reneker, *Advanced Materials* 16 (2004) 69.
- [10] C. Wang, M. Waje, X. Wang, J.M. Tang, R.C. Haddon, Y. Yan, *Nano Letters* 4 (2004) 345.
- [11] W.Z. Li, C. Liang, W. Zhou, J. Qiu, Z. Zhou, G. Sun, Q. Xin, *Journal of Physical Chemistry B* 107 (2003) 6292.
- [12] M.S. Saha, R. Li, X. Sun, S. Ye, *Electrochemistry Communications* 11 (2009) 438.
- [13] C.-C. Chen, C.F. Chen, C.-H. Hsu, I.-H. Li, *Diamond and Related Materials* 14 (2005) 770.
- [14] N. Rajalakshmi, H. Ryu, M.M. Shaijumon, S. Ramaprabhu, *Journal of Power Sources* 140 (2005) 250.
- [15] J.W. Jang, C.E. Lee, T.J. Lee, S.C. Lyu, C.J. Lee, *Current Applied Physics* 6 (2006) 141.
- [16] S.H. Lim, H.I. Elim, X.Y. Gao, A.T.S. Wee, W. Ji, J.Y. Lee, J. Lin, *Physical Review B* 73 (2006) 045402.
- [17] M. Shim, N. Wong, S. Kam, R.J. Chen, Y. Li, H. Da, *Nano Letters* 2 (2002) 285.
- [18] S. Bhattacharyya, C. Sinturel, J.-P. Salvetat, M.-L. Saboungi, *Applied Physics Letters* 86 (2005) 113104.
- [19] B.R. Azamian, J.J. Davis, K.S. Coleman, C.B. Bagshaw, M.L.H. Green, *Journal of the American Chemical Society* 124 (2002) 12664.
- [20] B.F. Erlanger, B.-X. Chen, M. Zhu, L. Brus, *Nano Letters* 1 (2001) 465.
- [21] S. Sotiropoulou, N.A. Chaniotakis, *Analytical and Bioanalytical Chemistry* 375 (2003) 103.
- [22] F. Villalpando-Páez, *Chemical Physics Letters* 386 (2004) 137.
- [23] F.A. Armstrong, H.A.O. Hill, N.J. Walton, *Accounts of Chemical Research* 21 (1988) 407.
- [24] Y.-Y. Horng, Y.-K. Hsu, A. Ganguly, C.-C. Chen, L.-C. Chen, K.-H. Chen, *Electrochemistry Communications* 11 (2009) 850.
- [25] Desriani, T. Hanashi, T. Yamazaki, W. Tsugawa, K. Sode, *The Open Electrochemistry Journal* 2 (2010) 6.
- [26] S. Kakhki, M.M. Barsan, E. Shams, C.M.A. Brett, *Synthetic Metals* 161 (2012) 2718.
- [27] X. Crispin, F.L.E. Jakobsson, A. Crispin, P.C.M. Grim, P. Andersson, A. Volodin, C. van Haesendonck, M. Van der Auweraer, W.R. Salaneck, M. Berggren, *Chemistry of Materials* 18 (2006) 4354.
- [28] D.W. Breiby, L.B. Samuelsen, B. Groenedaal, B. Struth, *Journal of Polymer Science Part B: Polymer Physics* 41 (2003) 945.
- [29] H. Liu, Y. Zhang, R. Li, X. Sun, D. Désilets, H. Abou-Rachid, *Carbon* 48 (2010) 1498.
- [30] M.E. Ghica, C.M.A. Brett, *Analytica Chimica Acta* 532 (2005) 145.
- [31] A. Guiseppi-Ellie, C. Lei, R.H. Baughman, *Nanotechnology* 13 (2002) 559.
- [32] L.L. Madsen, K. Carneiro, B.N. Zaba, A.E. Underhill, M.J. Van der Sluijs, *Synthetic Metals* 41–43 (1991) 2931.
- [33] R.C. Carvalho, C. Gouveia-Caridade, C.M.A. Brett, *Analytical and Bioanalytical Chemistry* 398 (2010) 1675.
- [34] D.J. Guo, H. Li, *Journal of Solid State Electrochemistry* 9 (2005) 445.
- [35] J. Bobacka, A. Lewenstam, A. Ivaska, *Journal of Electroanalytical Chemistry* 489 (2000) 17.
- [36] E. Barsoukov, J.R. Macdonald (Eds.), *Impedance Spectroscopy. Theory Experiment and Applications*, 2nd ed., Wiley, New York, 2005.
- [37] M. Liu, Y. Wen, D. Li, R. Yue, J. Xu, H. He, *Sensors and Actuators B* 159 (2011) 277.